Angewandte Chemie
Eine Zeitschrift der Gesellschaft Deutscher Chemiker

Supporting Information

Aptamer Blocking Strategy Inhibits SARS-CoV-2 Virus Infection

Miao Sun, Siwen Liu, Xinyu Wei, Shuang Wan, Mengjiao Huang, Ting Song, Yao Lu, Xiaonan Weng, Zhu Lin, Honglin Chen, Yanling Song,* and Chaoyong Yang**

anie_202100225_sm_miscellaneous_information.pdf

Supporting Information

69451 Weinheim, Germany

Abstract: The COVID-19 pandemic caused by SARS-CoV-2 is threating global health. Inhibiting interaction of the receptor-binding domain of SARS-CoV-2 S protein (S_{RBD}) and human ACE2 receptor is a promising treatment strategy. However, SARS-CoV-2 neutralizing antibodies are compromised by their risk of antibody-dependent enhancement (ADE) and unfavorably large size for intranasal delivery. To avoid these limitations, we demonstrated an aptamer blocking strategy by engineering aptamers' binding to the region on S_{RBD} that directly mediates ACE2 receptor engagement, leading to block SARS-CoV-2 infection. With aptamer selection against S_{RBD} and molecular docking, aptamer CoV2-6 was identified and applied to prevent, compete with, and substitute ACE2 from binding to S_{RBD}. CoV2-6 was further shortened and engineered as a circular bivalent aptamer CoV2-6C3 (cb-CoV2-6C3) to improve the stability, affinity, and inhibition efficacy. cb-CoV2-6C3 is stable in serum for more than 12 h and can be stored at room temperature for more than 14 days. Furthermore, cb-CoV2-6C3 binds to S_{RBD} with high affinity (K_d=0.13 nM) and blocks authentic SARS-CoV-2 virus with an IC_{50} of 0.42 nM.

SUPPORTING INFORMATION

Table of Contents

SUPPORTING INFORMATION

1. Materials and Methods

1.1 Reagents.

Protein A beads for Fc-tagged-RBD conjugation were purchased from Sino Biological Inc. (China). Streptavidin-coated sepharose beads used in SELEX and Ni beads for His-tagged RBD conjugation were from GE Healthcare (USA). Fc-tagged-RBD of SARS-CoV-2 Spike Protein (40592-V05H), His-tagged-RBD of SARS-CoV-2 Spike Protein (40592-V08B), SARS-CoV-2 Spike S1+S2 ECD-His recombinant protein (40589-V08B1), His-tagged-human ACE2 (10108-H08H), Fc-tagged human ACE2 (10108-H05H), biotin-goat anti-mouse IgG-Fc secondary antibody (SSA013), SARS-CoV spike -His recombinant protein (40150-V08B2), MERS-CoV spike-His recombinant protein (40069-V08H), human coronavirus HKU1 spike-His recombinant protein (40602-V08H), and HIV-1 gp120-His recombinant protein (40402-V08H) were purchased from Sino Biological Inc (China).

Human plasma and leukocyte were obtained from the volunteers' whole blood and handled within 24 hours. All the blood sample procedures were approved by the ethics committee of the First Affiliated Hospital of Xiamen University (KYX-2018-006). All DNA sequences were synthesized by Sangon Biotech with HPLC purification (Shanghai, China). The binding buffer (PBS, pH=7.4, including 136.8 mM NaCl, 10.1 mM Na_2HPO_4, 2.7 mM KCl, 1.8 mM KH_2PO_4, 0.55 mM $MgCl_2$), was used for aptamer selection and characterization. All media for cell culture were purchased from Gibco (USA). Fetal bovine serum (FBS) was obtained from PEAK (USA) and penicillin-streptomycin was obtained from Hyclone (USA).

1.2 Cells and pseudoviruses.

HEK-293T cells that stably express human ACE2 and SARS-CoV-2 Spike pseudotype HIV were obtained from Fubio Biotechnology Co., Ltd (Suzhou, China). SARS-CoV-2 Spike pseudotype HIV was packaged with spike protein of SARS-CoV-2 as a surface capsid glycoprotein by a lentivirus packaging system, and the RNA genome with the gene of CMV-promoter, GFP, IRES and luciferase (http://www.fubio.cn/cpzs_show.asp?ClassID1=1&ClassID=21&id=16). Cells were cultured in high glucose DMEM supplemented with 10% fetal bovine serum (FBS) and 1% penicillin-streptomycin solution at 37°C in a 5% CO_2 atmosphere. The pseudovirus used in the neutralization assay was stored at -80°C and the assay was performed in a BSL-2 laboratory.

1.3 SELEX procedures.

The SELEX procedure used in this work was performed as described in our previous work[1]. The single-strand DNA library included a 40-nt randomized sequence flanked by 18-nt sequences for PCR primer annealing and amplifying (5'- ATCCAGAGTGACGCAGCA - 40N - TGGACACGGTGGCTTAGT-3'). Initially, 5 nmol of ssDNA library was diluted in 500 μL binding buffer, and then annealed at 95°C, cooled on ice for 5 min, and slowly restored to room temperature. The SARS-CoV-2 RBD (Arg 319-Phe 541) expressed with the Fc region of mouse IgG1 at the C-terminus by HEK293 cells with post-modifications was conjugated to protein A-beads to form RBD-Protein A-beads as the target. RBD-Protein A-beads were incubated with the library at 25°C for 30 min, and then separated and washed twice with binding buffer. The recovered RBD-Protein A-beads were added to the PCR mixture (primers, dNTP, and EasyTaq DNA polymerase) to amplify the target bound sequences. Afterward, streptavidin-coated sepharose beads were utilized to bind the double strand amplification product, which was denatured in 0.1 M NaOH for 1 min to obtain a single-stranded library. After desalting with 3 K ultrafiltration tubes (Millipore), the new ssDNA pool was used for next round of selection. The concentrations of the resulting ssDNA pools were determined by UV-visible absorption (Nanodrop 1100, Thermo Fisher) at 260 nm. After 13 rounds of selection, the enriched libraries were subjected to high-throughput sequencing (Sangon Biotech, Shanghai, China).

Thirteen rounds of selection were performed, and the selection pressure was gradually increased as follows: 1) the amount of library input was reduced from 5 nmol to 200 pmol; 2) the amount of RBD protein input and the incubation time were decreased; 3) from 3 rounds of selection, protein A-beads and IgG-beads were used as the negative targets in counter selection; 4) after 6 rounds of selection, the selection target was replaced by S_{RBD} expressed by HEK293 cells with S_{RBD} expressed by baculovirus-insect cells; 5) from the ninth round of selection, 5 μg of ACE2 was added and incubated for 30 min, and the supernatant was collected for amplification.

1.4 Flow cytometry analysis.

To assess the enrichment of the ssDNA libraries during SELEX or the binding affinity of selected aptamers, positive RBD-Ni-beads (S_{RBD} expressed by insect cells) or negative Ni-beads were incubated with 200 nM FAM-labeled ssDNA libraries or the candidate sequences in 100 μL binding buffer at 25°C for 30 min. The beads were washed twice using binding buffer and suspended in 100 μL binding buffer. The fluorescence intensity of beads was measured by flow cytometry (FACSVerse, BD) by counting about 1000 events. To obtain the K_d value of the aptamers, a series of different concentration of aptamers with fluorescent labeling, ranging from 0 to 300 nM for CoV2-6 and CoV2-6C3 or 0 to 10 nM for circular bivalent aptamer, were incubated with 3 μL RBD-His-Ni beads (about 1.5 μg RBD protein). After 30 min incubation and washing twice using binding buffer, the mean fluorescence intensities analyzed by flow cytometry were recorded as Y and fitted to the equation $Y = B_{max} * X / (K_d + X)$ through Origin 8.0 software. The experiments for obtaining K_d were repeated as n= 3 independent replicates (Figure 2B and Figure 3E).

In the ACE2 prevention assay, 200 nM aptamer or control sequence was incubated with RBD-Ni-beads (S_{RBD} expressed by baculovirus - insect cells) at room temperature for 30 min. The beads were washed twice using binding buffer and resuspended in 200 μL binding buffer containing 20 ng Fc-tagged ACE2. After incubation with ACE2 for 1 h, the beads were washed twice and resuspended in 200 μL binding buffer containing biotin-goat anti-mouse IgG-Fc secondary antibody. After incubation for another 30 min, the beads were washed twice and resuspended in 200 μL binding buffer with SA-APC (Streptavidin-Allophycocyanin). In order to correct for non-specific adsorption by Ni-beads, the target beads incubated only with SA-APC were included as the background signal. After the final incubation and washing, the recovered beads were ready for flow cytometry analysis. In competition and substitution assay, except for changing the adding order of aptamer and ACE2, the experimental procedure was the same as above. The percentage of ACE2 prevention was calculated by the equation (1- (the fluorescence signal of the sample with the aptamer incubation - background signal) / (the fluorescence signal of the sample without the aptamer incubation - background signal)) *100%. Measurements were repeated as n = 3 independent replicates.

In the RBD neutralization assay, 200 nM aptamer or control sequence was incubated with 10 ng Fc-tagged RBD (S_{RBD} expressed by HEK293 cells) at room temperature for 30 min. After incubation, the mixtures were added to ACE2-Ni-beads and incubated for another 1 h at room temperature. The beads were washed twice and resuspended in 200 μL binding buffer containing biotin-goat anti-mouse IgG-Fc secondary antibody. After incubation of biotin-goat anti-mouse IgG-Fc secondary antibody, the beads were washed twice and incubated with SA-PE in 200 μL binding buffer. And all the samples were analyzed by flow cryometry. The target beads incubated only with SA-PE were also included as the background signal. The percentage of RBD neutralization was calculated by the equation (1- (the fluorescence signal of the sample with the aptamer incubation - background signal) / (the fluorescence signal of the sample without the aptamer incubation - background signal)) *100%. Half-maximal inhibitory concentration (IC_{50}) values for inhibition by aptamer of RBD binding to ACE2 was determined after log transformation of aptamer concentration using sigmoidal dose-response nonlinear regression analysis (Prism software, GraphPad Prism version 8.3.0). Assays were repeated as n = 3 independent replicates.

1.5 Fluorescence microscope imaging.

To assess the binding performance of selected aptamers, RBD-Protein A-beads (S_{RBD} expressed by HEK293 cells) were incubated with 200 nM FAM-labeled candidate sequences in 100 μL binding buffer at 25°C for 30 min. The beads were washed twice using binding buffer and suspended in 100 μL binding buffer. The fluorescence intensity of beads was measured by fluorescence microscope (Nikon). The K_d value of the aptamers were obtained from the fluorescence intensities of a series of different concentrations of ligands to the equation $Y = B_{max} * X / (K_d + X)$ through Origin 8.0 software.

1.6 Molecular docking and dynamic simulations.

The structure of SARS-CoV-2 S protein with a single RBD was obtained from the RCSB PDB data bank (http://www.rcsb.org, ID: 6VSB). The secondary structure with the minimum aptamer free energy was predicted by mfold web server (http://mfold.rna.albany.edu/?=mfold). Using the predicted secondary structure of the aptamer as a starting point, the corresponding 3D structures of the equivalent ssRNAs were then modeled and visualized in RNAcomposer. The 3D structures of candidate aptamers were then obtained by substituting bases T for U. Methyl groups were added to the C5 position of U. A refinement process was carried out based on molecular dynamics simulation (MDS) to relax the aptamer system.

Molecular docking was performed with Rosetta after obtaining the 3D structures of aptamers and their target. The Amber FF99SB and AMBER PARM99 force fields were used for the protein and aptamer system, respectively. The final average structure was obtained based on 5000 snapshots, which were extracted from the last 10 ns trajectory of MDS using the Gromacs 5.1 software[2].

1.7 Construction of circular bivalent aptamers.

To prepare the circular bivalent aptamer of CoV2-6C3, its two components (Table S3) were dissolved in T4 DNA Ligase buffer at a ratio of 1:1 and then heated at 95°C for 5 min, followed by rapid chilling to 16°C. Then, T4 DNA ligase (NEB, America) was quickly added to the solution and reacted at room temperature for 20 min. Afterwards, the T4 DNA ligase was denatured at 65°C for 10 min, according to the manufacturer's instructions. The concentration of cb-aptamer was determined by UV-Vis spectrometry. If necessary, aptamers were concentrated by 3K MWCO ultrafiltration centrifugation (Thermo Scientific).

1.8 Gel electrophoresis analysis of aptamer stability.

In the stability analysis in DMEM, 5 μM aptamers were incubated in DMEM containing 10% FBS at 37°C for 0, 6, 12, 24 and 48 h. At designated time points, samples were heated at 95°C for 10 min to denature the enzyme and subsequently stored at 4°C until all samples were collected.

In the stability analysis in plasma, 1 μM aptamers were incubated in plasma at 37°C for 0, 2, 4, 8 and 12 h. At designated time points, samples were heated at 95°C for 10 min to denature the enzyme and subsequently stored at 4°C until all samples were collected.

In the stability analysis of aptamers for long time at ambient temperature, 2 μM aptamers were collected at 0, 1, 3, 5, 7 and 14 days. Then, the DNA samples were loaded onto 8% polyacrylamide gel in 1×TBE buffer and run at 80 V for 40 min. After electrophoresis, the gels were analyzed with a molecular imager (BIO-RAD). The experiments for aptamer stability were repeated as n= 2 independent replicates (Figure 3B and Figure 3C).

1.9 Cell viability analysis.

ACE2-transfected 293T cells were seeded at a density of 1×10^4 in a 96-well plate. After 8-12 h cell culture, 0 or 500 nM circular bivalent aptamers were added to the monolayer cells. At 48 h after cell culture, cell viability was assessed using CCK-8 kit (Beyotime, China). The absorbance was read at 450 nm by a microplate reader (SpectraMax iDS). Cell viabilty assay was conducted six-times independent experiments.

1.10 Pseudovirus neutralization analysis.

To determine the neutralization ability of the aptamer, the pseudovirus neutralization assay was performed as previously described [3-4]. Serial dilutions of circular bivalent aptamer (1-1000 nM) and a control DNA sequence (1000 nM) in DMEM supplemented with 10% fetal bovine serum were pre-incubated with 5 μL 10^8 -10^9 copies/mL pseudoviruses per well for 1 h at 37°C, and then the mixtures were added to monolayer 10^4 ACE2-transfected 293T cells cultured in 96-well plates. Six hours after infection, culture medium was refreshed and then cells were cultured at 37°C for another 48 h. Then the original medium was removed and fresh medium supplemented with 0.2 mg/mL D-luciferin (100 uL/well) was added. After reaction at room temperature for 15 min, the luciferase activity was measured on a Multimode Plate Reader (SpectraMax iDS), and the resulting curves was analyzed by nonlinear regression to calculate the half-maximal inhibitory concentration (IC_{50}) values using Prism software version 8.3.0 (GraphPad). These experiments were repeated as n= 3 independent replicates.

The GFP expression in infected ACE2-transfected 293T cells were determined by fluorescence microscopy. Briefly, the 5 μL 10^8 -10^9 copies/mL pseudoviruses per well were incubated with different concentrations of aptamers (5 and 500 nM) or without aptamers for 1 h at 37°C. Then the mixtures were added to monolayer ACE2-transfected 293T cells cultured in 384-well plates. After 6 h cell culture, culture

medium was refreshed and then cells were cultured at 37°C for another 48 h. Finally, GFP fluorescence channel and bright field imaging were performed for each well. These experiments were repeated as n= 3 independent replicates.

1.11 Authentic viral neutralization assays.

Serial dilutions of aptamers were mixed with authentic viruses, incubated for 1 h at 37°C, and then added to previously-plated Vero E6 cells. After one-hour incubation, the supernatant was removed and replaced with 2 mL DMEM medium with 5% fetal bovine serum. After 48 h cell culture at 37°C, cells were homogenized in 100 μL RNAzol solution for further analysis. For viral mRNA (S gene) and host gene (GAPDH) were measured by quantitative PCR (RT-qPCR) using SYBR green premix Kit (Takara) according to its manual and gene expression were detected in Light Cycle 480 instrument (Roche). The relative copy number of viral mRNA level compared to the host gene mRNA was analyzed by nonlinear regression to calculate the IC_{50} value using Prism software version 8.3.0 (GraphPad). And for immunofluorescent staining assay, the infected cells were fixed and stained using an anti-SARS-CoV-2 S_{RBD} antibody for the virus and Hoechst dye for cell nucleus. These experiments were repeated as n= 3 independent replicates. The SARS-CoV-2 (GenBank: MT835143.1, https://www.ncbi.nlm.nih.gov/nuccore/MT835143) was isolated from the nasopharyngeal aspirate specimen of a patient with laboratory-confirmed COVID-19 approved by Institutional Review Board of The University of Hong Kong/Hospital Authority (UW 13-372).[5] All experiments involving live SARS-CoV-2 followed the approved standard operating procedures of the University of Hong Kong Biosafety Level-3 facility.

2. Supporting Figures and Tables

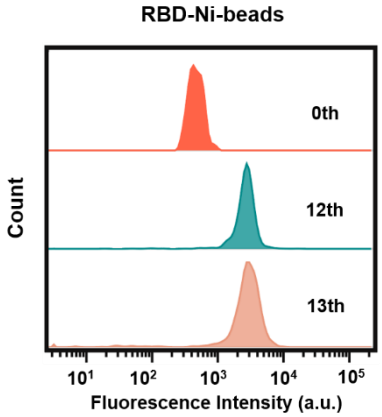

Figure S1. Flow cytometry to monitor the binding increments between 12th and 13th enriched pools with S_{RBD}. S_{RBD} was expressed by baculovirus-insect cells.

(A)

Family	7 th Percentage(%)	10 th Percentage(%)	13 th Percentage(%)	Representative Sequence
Family 1	0.068	11.742	67.289	CoV2-1
Family 2	0.015	0.147	17.601	CoV2-2
Family 3	0.015	1.685	8.975	CoV2-3
Family 4	0.015	0.266	6.169	CoV2-4
Family 5	72.382	74.060	3.315	CoV2-5
Family 6	17.140	11.120	0.194	CoV2-6
Family 7	0.405	0.532	0.131	CoV2-7
Family 8	0.764	0.414	0.080	CoV2-8

(B)

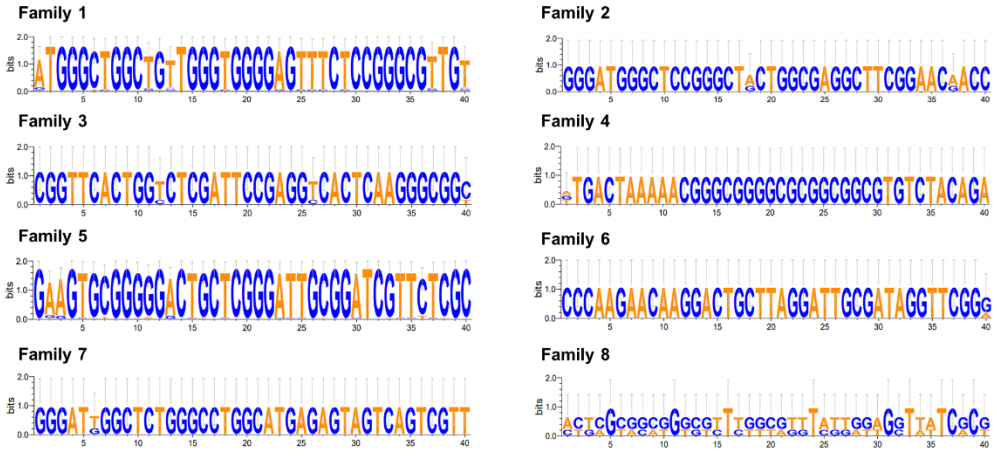

Figure S2. (A) The high-throughput sequencing results of 7th, 10th, 13th libraries. (B) The unique sequences (random fragment) of each family. The height of the symbols denotes the relative frequency of the nucleic acid.

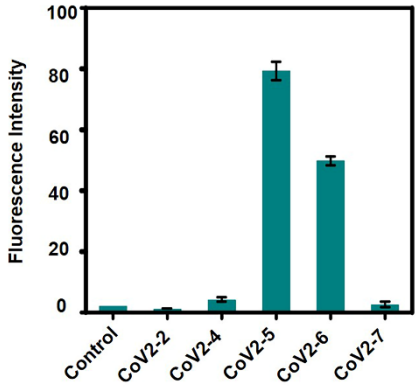

Figure S3. Characterization of the binding performance of selected aptamers targeting S_{RBD} expressed from HEK-293T cells.

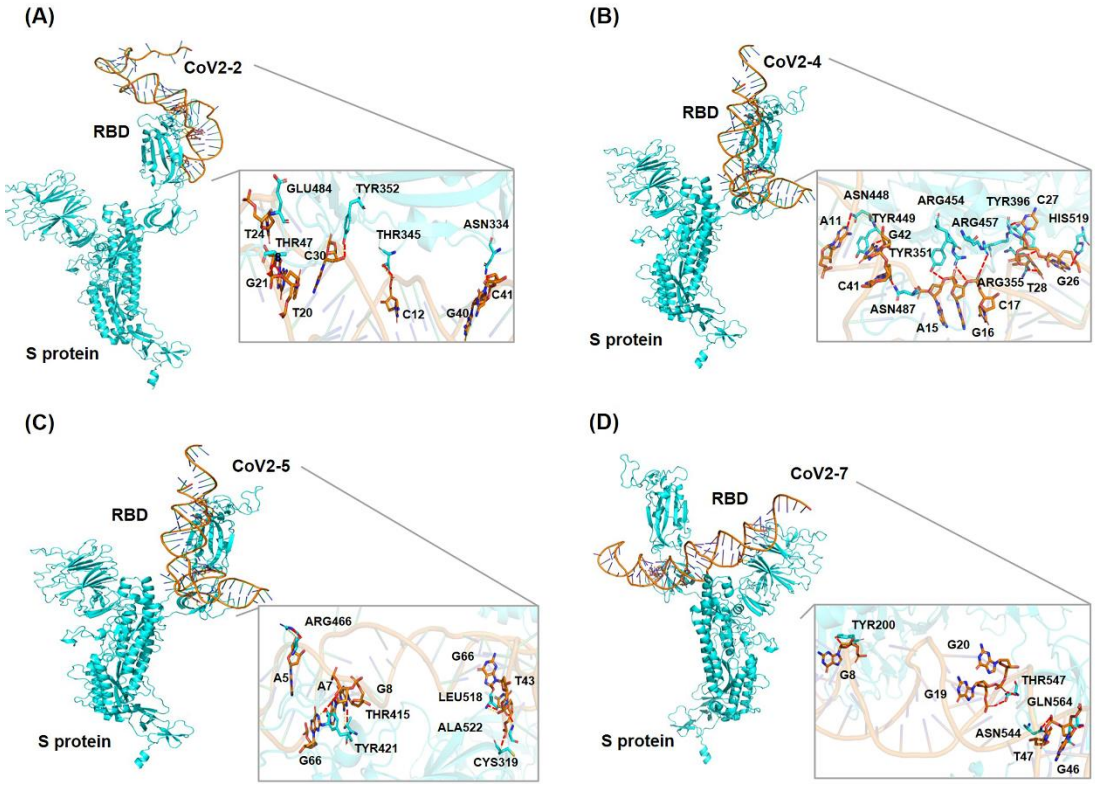

Figure S4. Docking complexes of the candidate aptamer (orange) and spike protein (cyan). Detailed analyses of the interface between (A-D) CoV2-2, CoV2-4, CoV2-5, CoV2-7 and RBD are shown in the corresponding enlarged images.

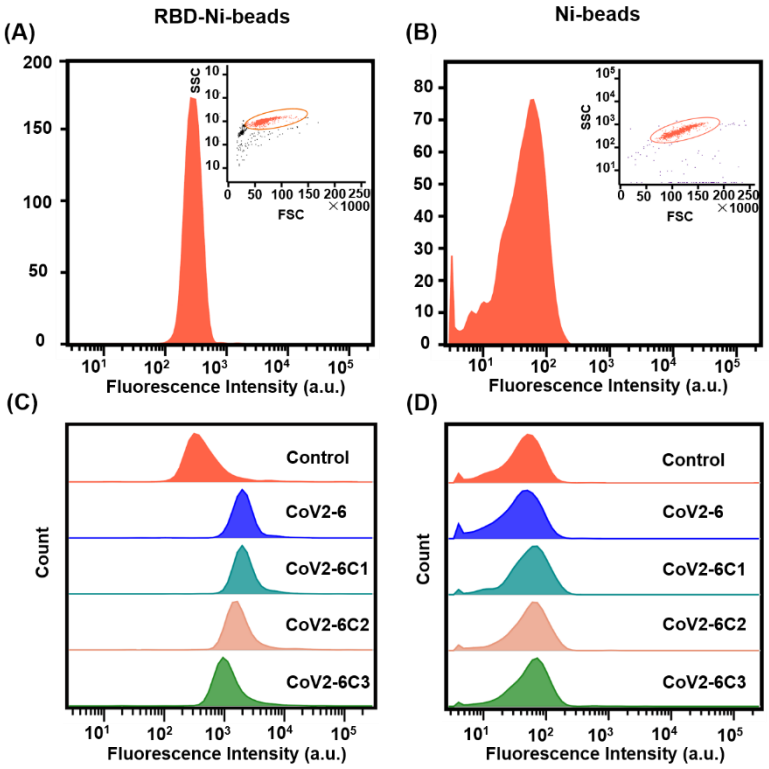

Figure S5. Flow cytometry analysis of (A) RBD-Ni-beads and (B) Ni-beads, insert figures are the histograms (FSC/SSC), respectively. Flow cytometry to investigate the binding performance of truncated sequences against (C) RBD-Ni-beads expressed by baculovirus-insect cells and (D) Ni-beads.

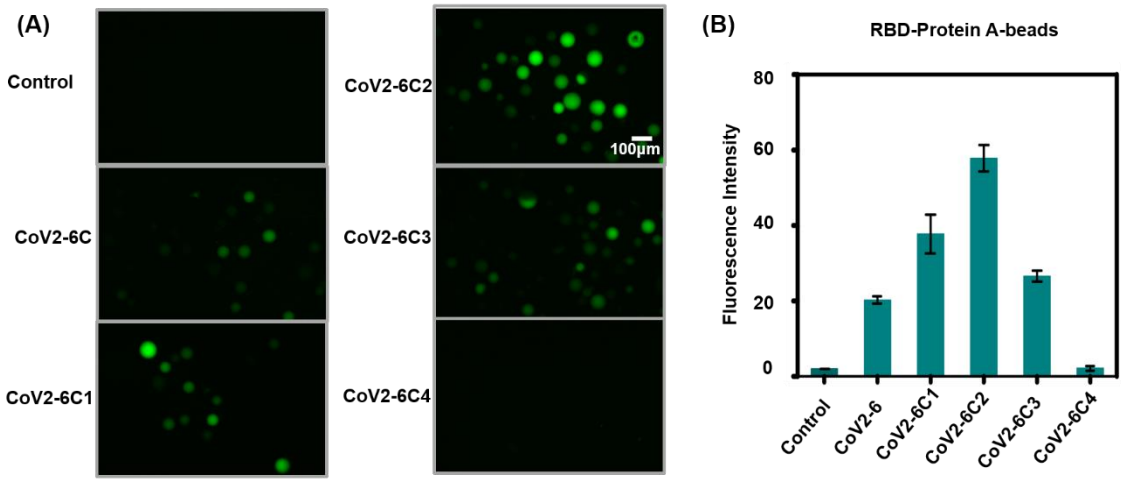

Figure S6. Fluorescent images to monitor the binding performance of truncated sequences to (A) RBD-Protein A-beads (RBD expressed from HEK293 cells) and (B) its fluorescence statistics.

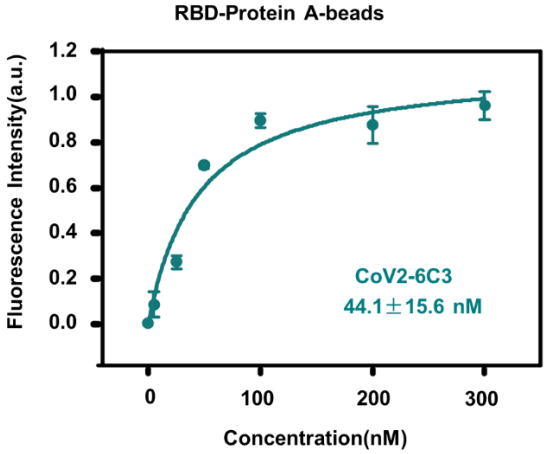

Figure S7. Binding curves of CoV2-6C3 against S_{RBD} expressed from HEK293 cells.

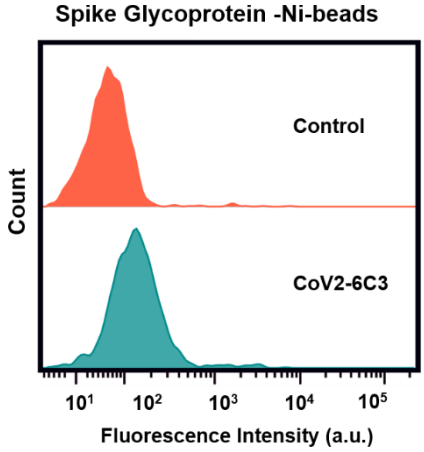

Figure S8. Flow cytometric analysis of CoV2-6C3 binding to SARS-CoV-2 Spike protein.

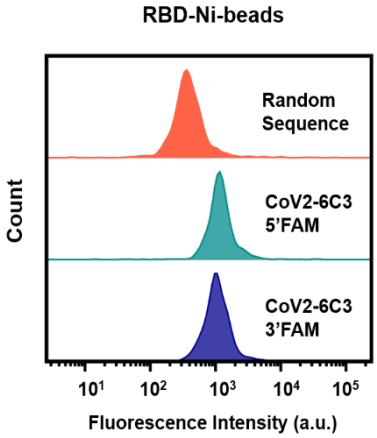

Figure S9. The binding performance of CoV2-6C3 with fluorescent label at the 5' or 3' ends to RBD-Ni-beads (expressed from baculovirus-insect cells).

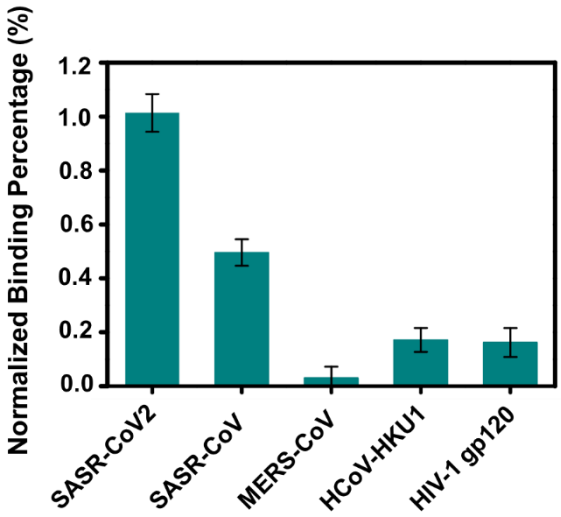

Figure S10. Selectivity study of CoV2-6C3 aptamer against the RBD/Spike protein (SARS-CoV, MERS-CoV, HCoV-HKU1) and key protein (HIV-1 gp120) of other viruses.

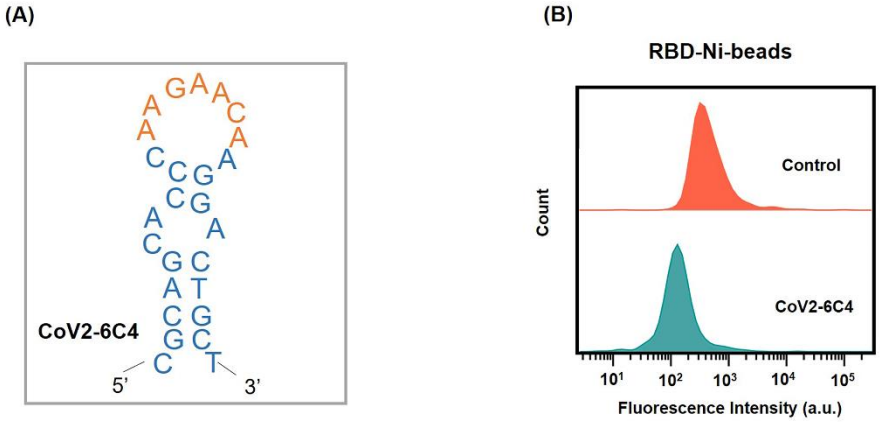

Figure S11. (A) The secondary structure of CoV2-6C4 simulated using the mfold software; bases in orange are predicted to interact with S_{RBD}. (B) Flow cytometry to investigate the binding performance of CoV2-6C4. S_{RBD} was expressed from baculovirus-insect cells.

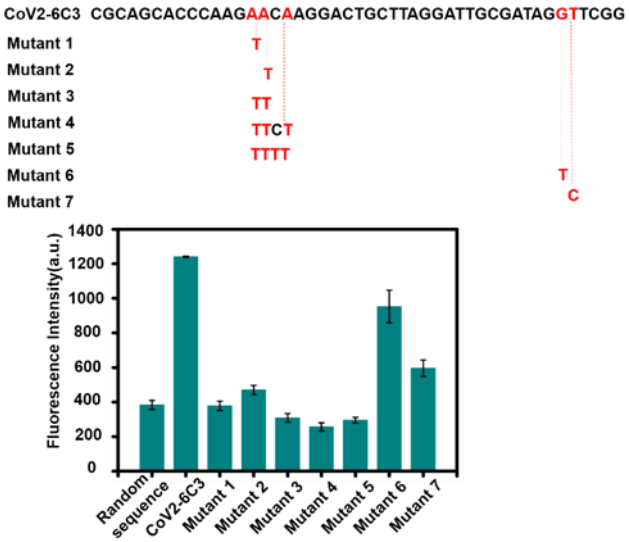

Figure S12. Binding performance of CoV2-6C3 aptamer and mutated aptamers against RBD-beads (expressed by baculovirus-insect cells).

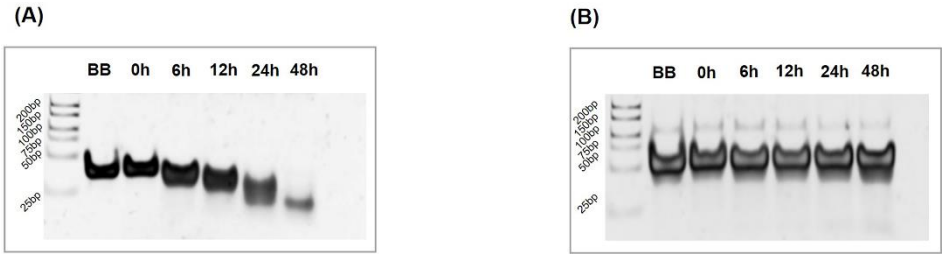

Figure S13. Stability analysis of (A) CoV2-6C3 and (B) circular bivalent CoV2-6C3 aptamer incubated with cell media (containing 10% FBS) at 37°C for different times.

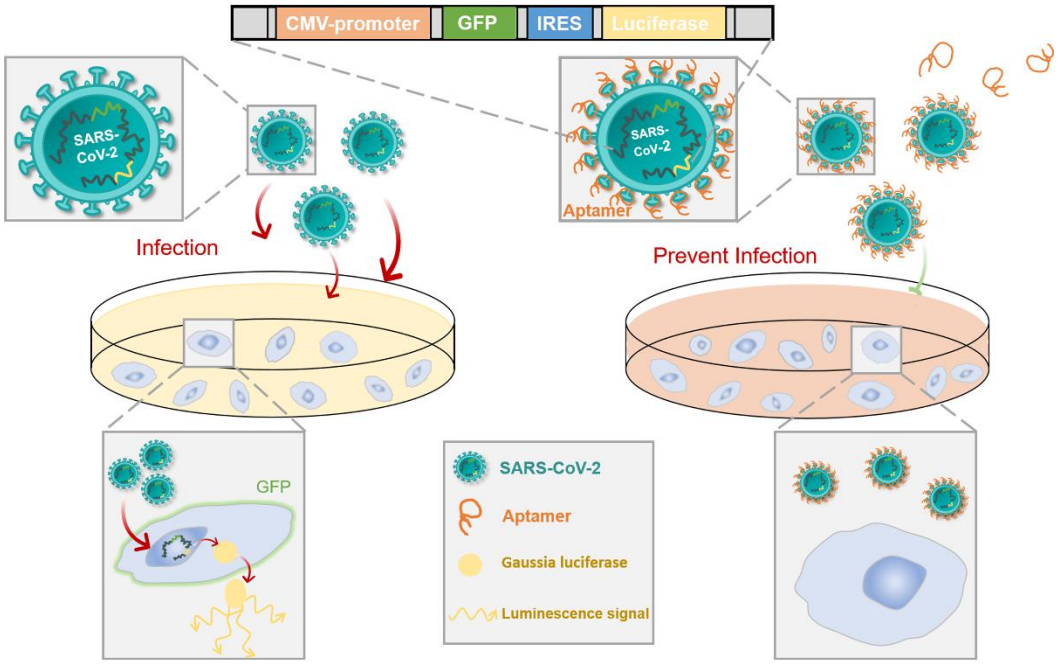

Figure S14. Schematic diagram of pseudovirus neutralization by circular bivalent CoV2-6C3 aptamer.

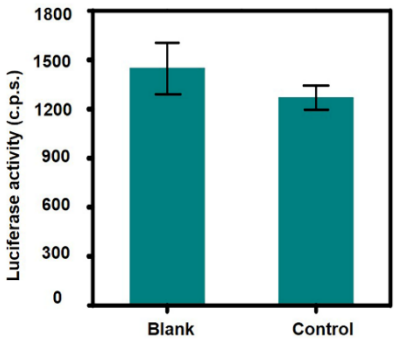

Figure S15. The inhibition activity of a control DNA sequence against pseudovirus infection.

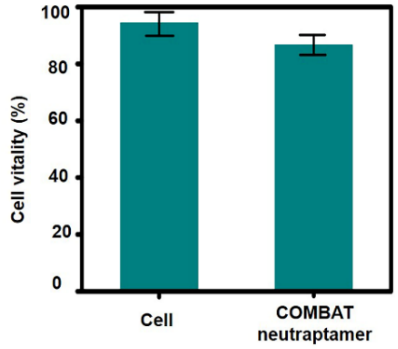

Figure S16. Examination of cell viability in the presence of circular bivalent CoV2-6C3 aptamer after 3 days treatment.

Table S1 the comparison of circular bivalent CoV2-6C3 aptamer and several reported neutralizing antibodies

Name	Viral protein binding K_d(RBD) (nM)	Inhibition kinetic (min^{-1})	Protein neutralization IC50 (μg/mL)	Pseudovirus neutralization IC50 (μg/mL)	Authentic virus neutralization IC50 (μg/mL) and inhibition efficacy		References
cb-CoV2-6C3	0.13	1.36	1.28	0.38	0.016	87%	This work
n3088	3.70	NA	NA	3.3	2.6	~80%	[6]
n3130	55.39	NA	NA	3.7	4.0	~60%	
1-20	NA	NA	NA	0.127	0.008	100%	[7]
2-38	NA	NA	NA	0.232	0.208	100%	
2-4	NA	NA	NA	0.394	0.057	100%	
2-30	MA	NA	NA	0.512	0.050	100%	
CV1	NA	NA	NA	15	NA	NA	[8]
CV30	3.6	NA	NA	0.03	NA	NA	
P2C-1A3	2.47	NA	NA	0.62	0.28	100%	[9]
S309	1.0×10^{-3}	NA	0.150	0.150	0.079	90%	[10]
VHH-72	38.6	23	NA	0.2	NA	NA	[11]
CA1	4.68±1.64	NA	NA	0.38	NA	NA	[12]
CB6	2.49±1.65	NA	NA	0.036	NA	NA	

Table S2 sequences of the selected aptamers

Name	Sequence (5'-3')
CoV2-1	**ATCCAGAGTGACGCAGCA**ATGGGCTGGCTGTTGGGTGGGGAGTTTCTCCGGGCGTTGT**GGACACGGTGGCTTAGTA**
CoV2-2	**ATCCAGAGTGACGCAGCA**GGGATGGGCTCCGGGCTACTGGCGAGGCTTCGGAACAACC**GGACACGGTGGCTTAGTA**
CoV2-3	**ATCCAGAGTGACGCAGCA**CGGTTCACTGGTCTCGATTCCGAGGTCACTCAAGGGCGGC**GGACACGGTGGCTTAGTA**
CoV2-4	**ATCCAGAGTGACGCAGCA**GTGACTAAAAACGGGCGGGGCGCGGCGGCGTGTCTACAGA**GGACACGGTGGCTTAGTA**
CoV2-5	**ATCCAGAGTGACGCAGCA**GAAGTGCGGGGGACTGCTCGGGATTGCGGATCGTTCTCGC**GGACACGGTGGCTTAGTA**
CoV2-6	**ATCCAGAGTGACGCAGCA**CCCAAGAACAAGGACTGCTTAGGATTGCGATAGGTTCGGG**GGACACGGTGGCTTAGTA**
CoV2-7	**ATCCAGAGTGACGCAGCA**GGGATGGGCTCTGGGCCTGGCATGAGAGTAGTCAGTCGTT**GGACACGGTGGCTTAGTA**
CoV2-8	**ATCCAGAGTGACGCAGCA**CTGAGTACATGTGTCTCTTTAGGTCGGATTGCTATTCACT**GGACACGGTGGCTTAGTA**
CoV2-6C1	**CGCAGCA**CCCAAGAACAAGGACTGCTTAGGATTGCGATAGGTTCGGG**GGACACGGTGGCTTAGTA**
CoV2-6C2	**ATCCAGAGTGACGCAGCA**CCCAAGAACAAGGACTGCTTAGGATTGCGATAGGTTCGG
CoV2-6C3	**CGCAGCA**CCCAAGAACAAGGACTGCTTAGGATTGCGATAGGTTCGG
CoV2-6C4	**CGCAGCA**CCCAAGAACAAGGACTGCT

Primer sequences are underlined.

Table S3 circular bivalent aptamers and their components

Name	Strand components(5'-3')
cb-CoV2-6C3	***P***-CGTAAATCAGTCACGCAGCACCCAAGAACAAGGACTG CTTAGGATTGCGATAGGTTCGG ***P***-TGACTGATTTACGCGCAGCACCCAAGAACAAGGACTG CTTAGGATTGCGATAGGTTCGG

Primer sequences are underlined. Green represents the FAM labeling.

3. References

[1] Y. Song, Z. Zhu, Y. An, W. Zhang, H. Zhang, D. Liu, C. Yu, W. Duan, C. J. Yang, *Anal. Chem.* **2013**, *85*, 4141.

[2] D. Van Der Spoel, E. Lindahl, B. Hess, G. Groenhof; A. E.Mark, H. J. Berendsen, *J. Comput. Chem*. **2005**, *26*, 1701.

[3] J. Pallesen, N. Wang, K. Corbett, D.Wrapp, R. Kirchdoerfer, H. Turner, C. Cottrell, M. Becker, L. Wang, W. Shi, *Proc. Natl. Acad. Sci*. **2017**,*114*, 7348.

[4] L. Wang, W. Shi, M. Joyce, K. Modjarrad, Y. Zhang, K. Leung, C. Lees, T. Zhou, H. Yassine, M. Kanekiyo, *Nat. Commun*. **2015**, 6, 7712.

[5] K. Kai-Wang To, O. Tak-Yin Tsang, C. Chik-Yan Yip, K.-Hung Chan, T.-Chiu Wu, J. Man-Chun Chan, W.-Shing Leung, T. Shiu-Hong Chik, C. Yau-Chung Choi, D. H. Kandamby, D. Christopher Lung, A. Raymond Tam, R. Wing-Shan Poon, A. Yim-Fong Fung, I. Fan-Ngai Hung, V. Chi-Chung Cheng, J. Fuk-Woo Chan, K.-Yung Yuen, *Clin. Infect. Dis.*, **2020**, *15*, 841.

[6] Y. Wu, C. Li, S. Xia, X. Tian, Y. Kong, Z. Wang, C. Gu, R. Zhang, C. Tu, Y. Xie, Z. Yang, L. Lu, S. Jiang, T.Ying, *Cell Host & Microbe* **2020**, 27, 891-898.

[7] L. Liu, P. Wang, S. Nair, J. Yu, M. Rapp, Q. Wang, Y. Luo, F.-W. Chan, V. Sahi, A. Figueroa, V. Guo, G. Cerutti, J. Bimela, J. Gorman, T. Zhou, Z. Chen, K. Yuen, D. Kwong, G. Sodroski, T. Yin, Z. Sheng, Y. Huang, L. Shapiro, D. Ho, *Nature* **2020**, *584*, 450.

[8] E. Seydoux, J. Homad, J. MacCamy, K. Rachael Parks, K. Hurlburt, F. Jennewein, R. Akins, B. Stuart, Yu-Hsin Wan, J. Feng, E. Whaley, S. Singh, M. Boeckh, W. Cohen, M. Juliana McElrath, A. Englund, Y. Chu, M. Pancera, T. McGuire, L. Stamatatos, *Immunity* **2020**, *53*, 98.

[9] B. Ju, Q. Zhang, J. Ge, R. Wang, J. Sun, X. Ge, J. Yu, S. Shan, B. Zhou, S. Song, X. Tang, J. Yu, J. Lan, J. Yuan, H. Wang, J. Zhao, S. Zhang, Y. Wang , X. Shi, L. Liu, J. Zhao, X. Wang, Z. Zhang, L. Zhang, *Nature* **2020**, *584*, 115.

[10] D. Pinto, Y. Park, M. Beltramello, C. Walls, M. Alejandra Tortorici, S. Bianchi, S. Jaconi, K. Culap, F. Zatta, A. De Marco, A. Peter, B. Guarino, R. Spreafico, E. Cameroni, J. Brett Case, E. Chen, C. Havenar-Daughton, G. Snell, A. Telenti, W. Virgin, A. Lanzavecchia, S. Diamond, K. Fink, D. Veesler, D. Corti, *Nature* **2020**, *583*, 290.

[11] D. Wrapp, D. De Vlieger, S. Corbett, M. Torres, N. Wang, W. Van Breedam, K. Roose, L. van Schie, M. Hoffmann, S. Pohlmann, S. Graham, N. Callewaert, B. Schepens, X. Saelens, S. McLellan, *Cell* **2020**, *181*, 1004.

[12] R. Shi, C. Shan, X. Duan, Z. Chen, P. Liu, J. Song, T. Song, X. Bi, C. Han, L. Wu, G. Gao, X. Hu, Y. Zhang, Z. Tong, W. Huang, J. Liu, G. Wu, B. Zhang, L. Wang, J. Qi, H. Feng, F. Wang, Q. Wang, F. Gao, Z. Yuan, J.Yan, *Nature* **2020**, *584*, 120.